PHYSICAL REVIEW A **91**, 011603(R) (2015)

Chromium dipolar Fermi sea

B. Naylor, A. Reigue, E. Maréchal, O. Gorceix, B. Laburthe-Tolra, and L. Vernac
Université Paris 13, Sorbonne Paris Cité, Laboratoire de Physique des Lasers, F-93430 Villetaneuse, France and CNRS, UMR 7538, LPL, F-93430 Villetaneuse, France
(Received 14 November 2014; published 20 January 2015)

We report on the production of a degenerate Fermi gas of ^{53}Cr atoms, polarized in the state $F = 9/2$, $m_F = -9/2$, by sympathetic cooling with bosonic $S = 3$, $m_S = -3$ ^{52}Cr atoms. We load in an optical dipole trap 3×10^4 ^{53}Cr atoms with 10^6 ^{52}Cr atoms. Despite the initial small number of fermionic atoms, we reach a final temperature of $T \simeq 0.6 \times T_f$ (Fermi temperature), with up to 10^3 ^{53}Cr atoms. This surprisingly efficient evaporation stems from an interisotope scattering length $|a_{BF}| = 80(\pm 10)a_B$ (Bohr radius) which is small enough to reduce evaporative losses of the fermionic isotope, but large enough to assure thermalization.

DOI: 10.1103/PhysRevA.91.011603 PACS number(s): 03.75.Ss, 37.10.De, 67.85.Pq

There has recently been tremendous activity on dipolar quantum gases. This is due to the fact that in dipolar gases the particles interact through long-range and anisotropic dipole-dipole interactions (DDIs), which drastically changes the nature of many-body ground and excited states. Following the seminal results with dipolar Bose-Einstein condensates of chromium [1,2], and then dysprosium [3] and erbium [4] atoms, the focus now turns towards dipolar degenerate Fermi gases, which raise fascinating prospects for the study of novel Fermi liquid properties [5], p-wave superconductivity [6], topological $px + ipy$ phases [7], or unconventional magnetism [8–11].

Dipolar Fermi gases of dysprosium [12] and erbium [13] have recently been produced, and a Fermi surface deformation induced by dipolar interactions was shown in [14]. However, the density of magnetically tunable Feshbach resonances in these lanthanide atoms is very large [15,16], due to anisotropic short-range interactions. As this density promises to be even higher in the context of spinor gases where more than one spin state is populated, study of magnetism might be difficult with these atoms. For this reason, chromium, with a combination of relatively strong dipole-dipole long-range anisotropic interactions and simple isotropic short-range interactions, remains a unique atom for the study of the unconventional spinor properties of dipolar quantum degenerate Fermi gases.

Despite its interest, producing a dipolar degenerate Fermi gas of chromium atoms has been elusive for many years, as it represents a real experimental challenge. The main reason is the small number of ^{53}Cr atoms that can be captured in a magneto-optical trap (MOT), at most typically 10^5, due to relatively small natural abundance, the complex hyperfine structure, and, most importantly, the very large light-assisted loss rate in a MOT [17]. In this Rapid Communication, we describe a method to produce quantum gases of fermionic ^{53}Cr atoms.

Our scheme consists of loading a mixture of most-abundant ^{52}Cr atoms and minority ^{53}Cr atoms in the same far-detuned optical dipole trap (ODT), and then performing forced evaporative cooling. Evaporative losses are smaller for ^{53}Cr atoms than for ^{52}Cr atoms, which results in very efficient evaporative cooling characterized by a gain of typically four orders of magnitude in phase-space density for one order of magnitude of atom losses. As a consequence, although only 3×10^4 ^{53}Cr atoms are loaded in the dipole trap at 60 μK before evaporation, degenerate Fermi gases of up to 10^3 atoms can be produced in less than 15 s. We analyze our evaporation scheme and are able to point out the decisive role played by the numerical value of the interisotope scattering length, which is smaller than the bosonic scattering length. We measure this quantity, and find a good agreement with theoretical predictions based on mass scaling [18].

Fermi statistics leads to vanishing s-wave collisions due to van der Waals interactions at low temperatures for polarized fermions. Therefore, evaporative cooling to degeneracy, which requires efficient thermalization, has been achieved either with a mixture of two fermionic Zeeman states [19] for which s-wave collisions are allowed, or for a Bose-Fermi mixture [20]. With dipolar species, low temperature collisions become possible even for identical fermions. This very peculiar consequence of DDIs, first observed with Dy [12], was used to produce an Er Fermi sea in a very efficient way [13]. However, for Cr the dipolar elastic cross section is $\simeq 20$ times smaller than for Er, as it scales as d^4m^2 (d being the permanent magnetic dipole, and m the mass). In addition, we only manage to trap in a conservative trap about 30 times less atoms than in [13], which is very unfavorable for a scenario involving only ^{53}Cr atoms. This is why we chose to perform sympathetic cooling with the bosonic ^{52}Cr.

We now describe the experimental setup used in this work with special focus on the lasers. The strategy we use to Bose condense ^{52}Cr is to accumulate atoms captured inside a MOT into a superimposed far-detuned ODT produced by a 100 W infrared (IR) fiber laser (at 1075 nm) [21]. To improve loading in the ODT we make use of optical pumping from excited ^7P states of the MOT trapping transition to different metastable states, in which they are protected from light-assisted collisions [17]. After the ODT is loaded, the MOT is turned off, atoms are repumped into the $^7S_3$ ground state, optically pumped to the absolute ground state $m_s = -3$, and finally transferred to a crossed ODT in which evaporation is performed.

To adapt this strategy to trap both isotopes in the same ODT, new laser lines are necessary due to the hyperfine structure of the fermionic isotope. The trapping laser frequencies needed to obtain a ^{53}Cr MOT using the $^7S_3 \rightarrow {}^7P_4$ transition at 425 nm were reported in [17]. They are generated from a

dedicated laser system producing 800 mW of 425 nm light. The optimal MOT for loading the ODT contains 10^5 ^{53}Cr atoms, at a temperature of 120 μK, close to the Doppler temperature. Atoms decay to metastable states $^5D_3, F = 9/2$ and $^5D_4, F = 11/2$ (from excited state $^7P_4, F = 11/2$), and $^5S_2, F = 7/2$ (from $^7P_3, F = 9/2$, see below). Repumping of these states to the ground state is performed via the excited state $^7P_3$ [22].

Optimization of the loading of the ODT with ^{52}Cr was studied in [23]. It revealed, in particular, the crucial role played by the metastable $^5S_2$ state, populated from the MOT by using a depumping beam at 427 nm (almost resonant with the $^7S_3 \rightarrow {}^7P_3$ transition). Optimal depumping allows double the atom number in the ODT. For the fermionic case, we could only increase the atom number by 20% when depumping to $^5S_2$. We interpret this reduction in efficiency as a result of significantly larger inelastic collisions between $^5S_2, F = 7/2$ ^{53}Cr atoms, compared to $^5S_2$ ^{52}Cr atoms. This may arise from the unfavorable "inverted" hyperfine structure in this state: Energetically allowed two-body inelastic collisions processes may populate the other hyperfine states of $^5S_2$, leading to losses. We finally could accumulate about 10^5 ^{53}Cr atoms in the ODT, compared with up to 2×10^6 for ^{52}Cr, with respective $1/e$ loading times equal to 200 and 50 ms.

In our experiment, the Zeeman slower beam used to decelerate ^{53}Cr substantially reduces the ^{52}Cr MOT atom number [17]. Therefore, we do not load the two isotopes concurrently in the ODT. Instead, we first make a ^{53}Cr MOT (to load ^{53}Cr atoms in the ODT), then switch off the blue beams specific to the ^{53}Cr MOT and turn on the ^{52}Cr MOT for a given amount of time Δt (to load ^{52}Cr atoms in the ODT). We then detect both atom numbers, N_B and N_F. Figure 1 shows that the presence of both isotopes in the ODT leads to losses, attributed to interisotope inelastic losses [22]. The starting point for evaporative cooling is therefore a trade-off: When Δt increases, N_B increases, but N_F decreases. With $\Delta t =$ 90 ms, we obtain the following optimal mixture for evaporation: $N_F = 3 \times 10^4$ and $N_B = 1 \times 10^6$.

Once the atoms are optically pumped to their absolute ground state (respectively, $S = 3, m_S = -3$ and $F = 9/2$, $m_F = -9/2$), the crossed dipole trap is implemented by transferring 80% of the IR power to a vertical beam in 9 s. The total IR power is then reduced to 1 W (starting at $t = 4$ s in Fig. 2) in 8 s. Figure 2 shows the evolution of the Boson temperature T_B and atom numbers for both isotopes. Thermalization between the two isotopes is relatively good during the whole evaporation process as shown by Fig. 3. Consequently, the interspecies cross section σ_{BF} has to be relatively large. On the other hand, thermalization is not perfect: T_F is measured to be about 20% higher than T_B. We thus infer that σ_{BF} is smaller than the bosonic cross section σ_{BB}. At the end of the ramp, a ^{52}Cr BEC is obtained with typically 10^4 atoms, while N_F ranges between 500 and 1000.

The power of the IR laser is then rapidly ramped up (to 5 W) to obtain a tighter trap and freeze evaporation. Trap frequencies $\omega_{x,y,z} = 2\pi \times (430,510,350)$ Hz are measured through parametric excitation, with 5% uncertainty. In this trap, we calculate the critical temperature for BEC, $T_c = 380$ nK for 10^4 atoms, and the Fermi temperature, $T_f = 370$ nK for 10^3 atoms. The experimental temperatures are obtained by fitting

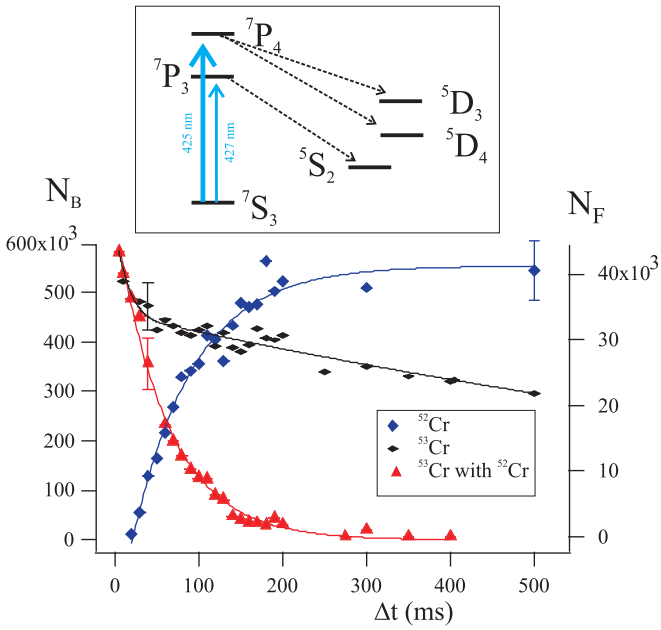

FIG. 1. (Color online) Inelastic interspecies collisions in the ODT. The lifetime of ^{53}Cr atoms in the ODT dramatically drops when ^{52}Cr atoms are loaded starting at $t = 0$. This sets a tight constraint to optimize loading before sympathetic cooling. Solid lines are fit to the data, using exponential functions. Error bars show statistical uncertainties. Inset: chromium energy levels of interest.

the velocity distributions imaged after a free fall, by a bimodal distribution for ^{52}Cr, and by either [24] a Boltzmann or a Fermi-Dirac distribution for ^{53}Cr. We obtain $T_B = (180 \pm 20)$ nK and $T_F = (220 \pm 20)$ nK. We therefore obtain $T_F/T_f = 0.6 \pm 0.08$.

In addition to reporting the production of ^{53}Cr degenerate gases, one of the main points of this Rapid Communication is to explain why our strategy to reach quantum degeneracy is efficient despite the small atom number before evaporation. For that we develop the following theoretical model, based

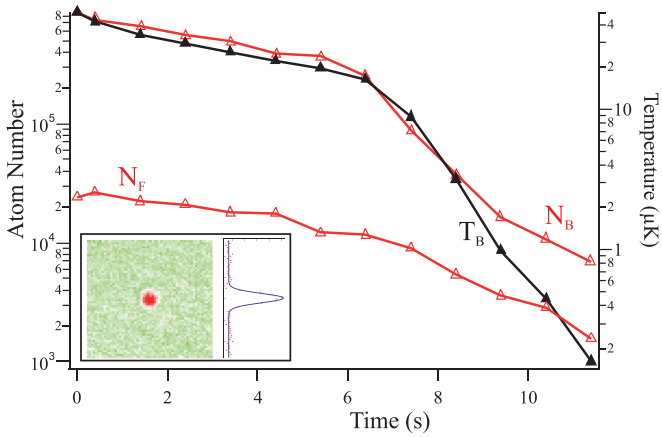

FIG. 2. (Color online) Time evolution of ^{52}Cr temperature (T_B) and atom number of both isotopes during evaporation. The crossed dipole trap is fully loaded at $t = 7$ s. The evaporation ends at $t = 12$ s. Inset: *in situ* absorption image of a degenerate fermionic ^{53}Cr cloud of 10^3 atoms, with corresponding integrated optical depth.

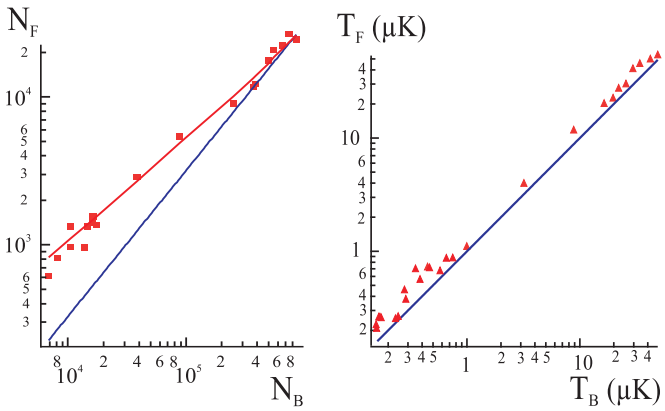

FIG. 3. (Color online) Comparison between the two isotopes during evaporation. Left: Atom numbers showing the smaller losses for fermions. The (red) curve is the prediction from Eq. (2); the straight (blue) line assumes constant ratio between atom numbers. Right: Temperatures. The temperature of the fermion remains about 20% higher than that of the boson during the whole sequence. The straight (blue) line corresponds to identical temperatures.

on the scaling laws for evaporation first introduced in [25]. Our main assumption is that polarized ^{53}Cr atoms only collide with ^{52}Cr atoms. This assumption is first motivated by the fact that the centrifugal barrier is of the order of 1 mK for the p-wave channel, much larger than the initial temperature of the cloud. As a consequence, polarized fermions can be considered not to collide with each other through van der Waals interactions. In addition, the expected scattering cross section between identical fermions due to DDIs, estimated to be 9.8×10^{-18} m^{-2} using first order Born approximation [26], is small enough that dipolar collisions may be neglected given the density. Therefore one can consider that fermions only collide with the more abundant ^{52}Cr atoms. Due to large differences in atom numbers, we assume as well that evaporative losses of bosons solely come from collisions with bosons.

Given these assumptions, the rate equations for evaporation read:

$$\begin{aligned}
\frac{dN_B}{dt} &= -\sigma_{BB} n_B \bar{V}_{BB} f(\eta_B) N_B - \Gamma N_B, \\
\frac{dN_F}{dt} &= -\sigma_{BF} n_B \bar{V}_{BF} f(\eta_F) N_F - \Gamma N_F, \\
\frac{d(3N_B T_B)}{dt} &= -\sigma_{BB} n_B \bar{V}_{BB} f(\eta_B)(\eta_B + 1) N_B T_B - 3\Gamma N_B T_B, \\
\frac{d(3N_F T_F)}{dt} &= -\sigma_{BF} n_B \bar{V}_{BF} f(\eta_F)(\eta_F + 1) N_F T_F - 3\Gamma N_F T_F,
\end{aligned} \tag{1}$$

where $i = B, F$ stands for boson or fermion, N_i for atom number, and n_i for average density; $\bar{V}_{ij} = [8k_B(m_i T_j + m_j T_i)/\pi m_i m_j]^{1/2}$ is the mean of the magnitude of the relative velocity, Γ is the one-body loss coefficient, independently measured to be $\Gamma = 0.1$ s^{-1}, η is the ratio between the trap depth and the thermal energy, and $f(\eta)$ is given for $\eta > 4$ by Eq. (11) of [27]. These equations assume thermal equilibrium. As noticed above the fermion temperature is slightly higher than the boson temperature, which signals a slight departure from thermal equilibrium. To interpret our data, we therefore assume thermal equilibrium for each gas, at a temperature which slightly depends on the isotope.

The first term on the right-hand side of each equation in Eq. (1) describes evaporation. One major difficulty in applying this model to quantitatively describe evaporation is that the rate of evaporation depends exponentially on η, via the exponential term in f. It is usually difficult to precisely measure the trap depth in one experiment (e.g., due to uncertainties in estimating waists of laser beams *in situ*). However, the trap depth is almost identical for the two isotopes (isotopic shifts being much smaller than the detunings of the IR laser to all optical transitions). In our analysis, we therefore strongly reduce the sensitivity to the trap depth by comparing the rate of evaporation of fermions to that of bosons. Assuming that η_i are constant in time, integrating the first two equations of (1) gives

$$\frac{\log_e\left(\frac{N_B(t_2)}{N_B(t_1)}\right) + \Gamma(t_2 - t_1)}{\log_e\left(\frac{N_F(t_2)}{N_F(t_1)}\right) + \Gamma(t_2 - t_1)} = \frac{\sigma_{BB}}{\sigma_{BF}} \times \frac{\bar{V}_{BB}}{\bar{V}_{BF}} \times \frac{f(\eta_B)}{f(\eta_F)}. \tag{2}$$

As seen from Eq. (2), the sensitivity to trap depth is not completely suppressed by the relative measurement, because the temperatures of both clouds are slightly different, leading to values of η_B and η_F differing by up to 20%. We therefore first estimate the value of η_B by comparing the measured loss rate of bosons and cooling rate. From the first and third equations in (1) we infer

$$\log_e\left(\frac{T_B(t_2)}{T_B(t_1)}\right) = \frac{2 - \eta}{3}\left[\log_e\left(\frac{N_B(t_1)}{N_B(t_2)}\right) - \Gamma(t_2 - t_1)\right]. \tag{3}$$

The analysis of our data using Eq. (3) leads to an experimental estimate of $\eta_B = 6.5 \pm 0.5$, which justifies the assumption made on the constancy of η_i. This value is in relatively good agreement with the value ≈ 7 which we infer from calibrating the trap depth. Using $T_F = 1.2\ T_B$, we find $f(\eta_F)/f(\eta_B) = 2.1 \pm 0.3$.

We now use our experimental data to estimate from Eq. (2) the value for the cross section σ_{BF}. We can use different portions of the experimental data to measure the ratio σ_{BF}/σ_{BB} as shown in Fig. 4. In practice, we span the times t_1 and t_2 over the range of experimental times. Experimental values of σ_{BF}/σ_{BB} all lie in the interval 0.31 ± 0.05 regardless of the choice of t_1 and t_2. This indicates that σ_{BF}/σ_{BB} is insensitive to temperature to within signal to noise. This is in good agreement with the assumptions that atoms collide mostly through s-wave and short-range interactions, and with theoretical predictions [28].

An outcome of our analysis is the first measurement of the boson-fermion scattering length a_{BF} in the $S = 6$ electronic molecular potential (both atoms being in the stretched state of lowest energy). Indeed, $\sigma_{BF} = 4\pi a_{BF}^2$ describes collisions between (distinguishable) bosons and fermions, while the value of $\sigma_{BB} = 8\pi a_{BB}^2$, which describes collisions between (undistinguishable) bosons, has been measured with accuracy [29]. In Fig. 4 we report the measured value of $a_6 = 102.5 a_B$ for ^{52}Cr [29], the less well known value for ^{50}Cr [30], as well as our newly measured value for $|a_{BF}| = 80(\pm 10) a_B$. The good agreement with predictions based on mass scaling [18] indicates that $a_{BF} > 0$, and shows that this theoretical

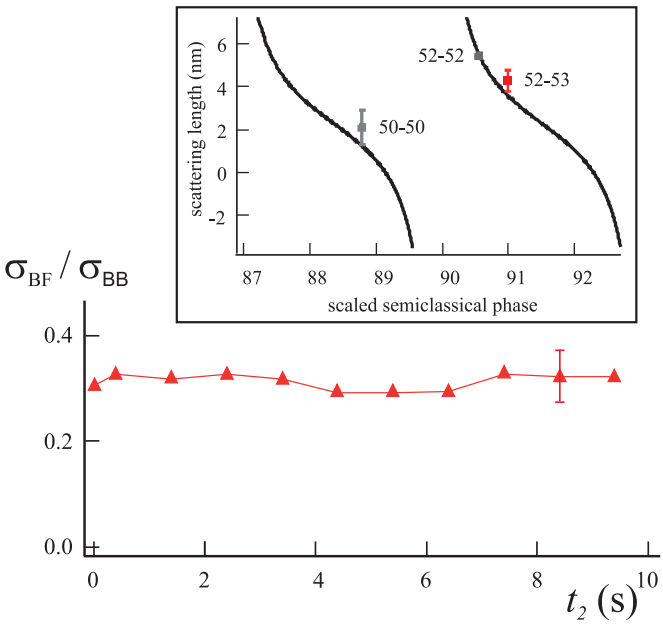

FIG. 4. (Color online) Experimental measurements of the ratio of the boson-boson and interisotope cross sections obtained using Eq. (2), with $t_1 = 10$ s (see text). The error bar shows the systematic uncertainty associated with $\eta_{B,F}$, which dominates over statistical uncertainties. Inset: scattering lengths of Cr, including a_{52-53} (this work). The solid line is the predicted scattering length using mass scaling of semiclassical phase [18].

approach remains valid despite the complexity of Cr_2 molecules.

Our analysis therefore confirms that $\sigma_{BF} < \sigma_{BB}$. As evaporation is optimized to be achieved as fast as possible for the boson, it is not surprising that the Fermi cloud lags slightly behind in terms of temperature. This analysis shows that our strategy to cool fermions is efficient because (i) σ_{BF} is sufficiently large to (almost) ensure interisotope thermal equilibrium; (ii) σ_{BF} is small enough to reduce evaporative losses of fermions, which leads to a gradual increase of the ratio of the number of fermions to the number of bosons as evaporation proceeds (see Fig. 3). This increase is essential for the positive outcome of our experiment.

In conclusion, we have produced a ^{53}Cr degenerate Fermi gas, with up to 10^3 atoms, together with a BEC of 10^4 ^{52}Cr atoms. This boson-fermion degenerate mixture might have peculiar properties, due to the strong imbalance in atom numbers. The spatial mode of the Fermi sea may be deformed by repulsive interaction with the BEC, which is of the order of the Fermi energy. Deformation of the Fermi surface may arise as well. These effects should be amplified close to an interisotope Feshbach resonance.

We plan to reveal the dipolar nature of the Cr Fermi sea by studying Pauli paramagnetism at low magnetic field. Quantum statistics is expected to lead then to a very different picture than that obtained for ^{52}Cr [31]. In a three-dimensional optical lattice, ^{53}Cr should provide a good platform even at relatively high T/T_f to study nonequilibrium dynamics associated with XYZ spin models [9], complementary to recent studies with ^{52}Cr [32].

LPL is Unité Mixte (UMR 7538) of CNRS and of Université Paris 13, Sorbonne Paris Cité. We thank A. Simoni for exchanges about mass scaling. We acknowledge financial support from Conseil Régional d'Ile-de-France under DIM Nano-K/IFRAF, CNRS, and from Ministère de l'Enseignement Supérieur et de la Recherche within a CPER contract.

[1] A. Griesmaier, J. Werner, S. Hensler, J. Stuhler, and T. Pfau, Phys. Rev. Lett. **94**, 160401 (2005).

[2] T. Koch, T. Lahaye, J. Metz, B. Fröhlich, A. Griesmaier, and T. Pfau, Nat. Phys. **4**, 218 (2008); T. Lahaye, J. Metz, B. Fröhlich, T. Koch, M. Meister, A. Griesmaier, T. Pfau, H. Saito, Y. Kawaguchi, and M. Ueda, Phys. Rev. Lett. **101**, 080401 (2008); G. Bismut, B. Pasquiou, E. Maréchal, P. Pedri, L. Vernac, O. Gorceix, and B. Laburthe-Tolra, *ibid.* **105**, 040404 (2010); G. Bismut, B. Laburthe-Tolra, E. Maréchal, P. Pedri, O. Gorceix, and L. Vernac, *ibid.* **109**, 155302 (2012).

[3] M. Lu, N. Q. Burdick, S. H. Youn, and B. L. Lev, Phys. Rev. Lett. **107**, 190401 (2011).

[4] K. Aikawa, A. Frisch, M. Mark, S. Baier, A. Rietzler, R. Grimm, and F. Ferlaino, Phys. Rev. Lett. **108**, 210401 (2012).

[5] M. A. Baranov, M. Dalmonte, G. Pupillo, and P. Zoller, Chem. Rev. **112**, 5012 (2012).

[6] M. A. Baranov, M. S. Marenko, V. S. Rychkov, and G. V. Shlyapnikov, Phys. Rev. A **66**, 013606 (2002).

[7] J. Levinsen, N. R. Cooper, and G. V. Shlyapnikov, Phys. Rev. A **84**, 013603 (2011).

[8] D. Peter, S. Muller, S. Wessel, and H. P. Büchler, Phys. Rev. Lett. **109**, 025303 (2012).

[9] M. L. Wall, K. Maeda, and L. D. Carr, arXiv:1410.4226.

[10] A. W. Glaetzle, M. Dalmonte, R. Nath, C. Gross, I. Bloch, and P. Zoller, arXiv:1410.3388.

[11] D. Peter, N. Y. Yao, N. Lang, S. D. Huber, M. D. Lukin, and H. P. Büchler, arXiv:1410.5667.

[12] M. Lu, N. Q. Burdick, and B. L. Lev, Phys. Rev. Lett. **108**, 215301 (2012).

[13] K. Aikawa, A. Frisch, M. Mark, S. Baier, R. Grimm, and F. Ferlaino, Phys. Rev. Lett. **112**, 010404 (2014).

[14] K. Aikawa, S. Baier, A. Frisch, M. Mark, C. Ravensbergen, and F. Ferlaino, Science **345**, 1484 (2014).

[15] A. Frisch, M. Mark, K. Aikawa, F. Ferlaino, J. L. Bohn, C. Makrides, A. Petrov, and S. Kotochigova, Nature (London) **507**, 475 (2014).

[16] K. Baumann, N. Q. Burdick, M. Lu, and B. L. Lev, Phys. Rev. A **89**, 020701(R) (2014).

[17] R. Chicireanu, A. Pouderous, R. Barbé, B. Laburthe-Tolra, E. Maréchal, L. Vernac, J.-C. Keller, and O. Gorceix, Phys. Rev. A **73**, 053406 (2006).

[18] G. F. Gribakin and V. V. Flambaum, Phys. Rev. A **48**, 546 (1993); V. V. Flambaum, G. F. Gribakin, and C. Harabati, *ibid.* **59**, 1998 (1999).

[19] B. DeMarco and D. S. Jin, Science **285**, 1703 (1999).

[20] A. G. Truscott, K. E. Strecker, W. I. McAlexander, G. B. Patridge, and R. G. Hulet, Science **291**, 2570 (2001); F. Schreck, L. Khaykovich, K. L. Corwin, G. Ferrari, T. Bourdel, J. Cubizolles, and C. Salomon, Phys. Rev. Lett. **87**, 080403 (2001).

[21] A. de Paz, B. Naylor, J. Huckans, A. Carrance, O. Gorceix, E. Maréchal, P. Pedri, B. Laburthe-Tolra, and L. Vernac, Phys. Rev. A **90**, 043607 (2014).

[22] Analysis of the loading optimization, as well as technical details of the experiment, and spectroscopic data of repumping lines, will be presented in a forthcoming paper.

[23] G. Bismut, B. Pasquiou, D. Ciampini, B. Laburthe-Tolra, E. Maréchal, L. Vernac, and O. Gorceix, Appl. Phys. B **102**, 1 (2011).

[24] For $T/T_F = 0.6$, it is expected that fitting the Fermi-Dirac distribution by the Boltzmann statistics leads to the same value of temperature within 3% (B. DeMarco, Ph.D. thesis, University of Colorado, 2001).

[25] K. M. O'Hara, M. E. Gehm, S. R. Granade, and J. E. Thomas, Phys. Rev. A **64**, 051403(R) (2001).

[26] S. Hensler, J. Werner, A. Griesmaier, P. O. Schmidt, A. Görlitz, T. Pfau, S. Giovanazzi, and K. Rzazewski, Appl. Phys. B **77**, 765 (2003).

[27] R. de Carvalho and J. Doyle, Phys. Rev. A **70**, 053409 (2004).

[28] A. Simoni (private communication).

[29] B. Pasquiou, G. Bismut, Q. Beaufils, A. Crubellier, E. Maréchal, P. Pedri, L. Vernac, O. Gorceix, and B. Laburthe-Tolra, Phys. Rev. A **81**, 042716 (2010).

[30] J. Werner, A. Griesmaier, S. Hensler, J. Stuhler, T. Pfau, A. Simoni, and E. Tiesinga, Phys. Rev. Lett. **94**, 183201 (2005).

[31] B. Pasquiou, E. Maréchal, L. Vernac, O. Gorceix, and B. Laburthe-Tolra, Phys. Rev. Lett. **108**, 045307 (2012).

[32] A. de Paz, A. Sharma, A. Chotia, E. Maréchal, J. H. Huckans, P. Pedri, L. Santos, O. Gorceix, L. Vernac, and B. Laburthe-Tolra, Phys. Rev. Lett. **111**, 185305 (2013).